New recombination centers in MBE MCT layers on (013) GaAs substrates

© S.A. Dvoretsky[1], M.F. Stupak[2], N.N. Mikhailov[1], V.S. Varavin[1], V.G. Remesnik[1],
S.N. Makarov[2], A.G. Elesin[2], A.G. Verhoglyad[2]

[1] Institute of Semiconductor Physics SB RAS,
Novosibirsk, Russia
[2] Technological Design Institute of Scientific Instrument Engineering at the Siberian Branch
of the Russian Academy of Sciences (TDI SIE SB RAS),
Novosibirsk, Russia

E-mail: dvor@isp.nsc.ru

A large inhomogeneity of the minority lifetime from 1 to $10\,\mu$s at $77\,$K over the area is observed in some experiments when high-quality HgCdTe layers of the electronic type of conductivity are grown on GaAs substrates with a diameter of $76.2\,$mm with the (013) orientation by the method of molecular beam epitaxy. As a rule, the such lifetimes are determined by carrier recombination at Shockley−Hall−Read (SHR) centers. Modern studies and ideas about the nature of the SHR centers do not allow us to explain the observed results. The measurements of HgCdTe layers by the second harmonic generation showed the existence of a quasi-periodic change in the signal at the minima of the azimuthal dependence, which is associated with the appearance of misoriented microregions of the crystal structure. The amplitude of the quasi-periodic change in the signal decreases with increasing lifetime and completely disappears for regions with higher lifetime values. Similar dependences are observed during etching of HgCdTe layers, which indicates the existence of misoriented microregions in the bulk. Thus, misoriented microregions of the crystal structure have a significant effect on the lifetime and are new centers of Shockley−Hall−Read recombination.

Keywords: HgCdTe layers, lifetime, second harmonic, azimuthal angular dependences, recombination centers, misoriented microregions.

1. Introduction

The heteroepitaxial structures (HES) of the solid solution of mercury and cadmium telluride (MCT, HgCdTe), being grown by the molecular beam epitaxy (MBE) method, take a leading position as a basic photo-sensitive material for the IR detectors with high sensitivity within the wide spectrum range of the wavelengths [1]. Currently, three main methods of epitaxial growth are used for growing HgCdTe: liquid-phase epitaxy (LPE), vapor-phase epitaxy from organometallic compounds (MOVPE, MOCVD) and molecular beam epitaxy (MBE). The MOVPE and MBE methods of growing the HES MCT on large-area substrates provide more homogeneous material characteristics, which is necessary to improve the performance and quality of signal reception, as well as obtaining complex structures with sharp and complex composition and doping throuhjout the thickness for the development of new detector designs. The MBE technology has been widely developed and is considered as the main direction for the growth of the HES MCT, including for industrial production at GaAs and Si substrates. This is due to a number of advantages of this technology over other epitaxial methods [2]. The quality of the MBE technology is determined by the quality of the HES MCT material and its characteristics at cryogenic

temperatures. After growing the HES MCT MBE without intentional doping have an electronic type (*n*-type) with high electrophysical characteristics: low concentration and high mobility of the major charge carriers, as well as a long lifetime (LT) of minor carriers. For IR-detectors with high parameters limited by background radiation, based on the material $Hg_{1-x}Cd_xTe$ with the composition of cadmium telluride $X_{CdTe} = 0.2-0.3$ requires cooling to cryogenic temperatures (liquid nitrogen temperatures and below). The undoped layers of the HES MCT MBE of high quality allow the manufacture of highly sensitive photoconductive IR-detectors [3–6]. Indium-doped (In) layers of the HES MCT MBE *n*-type with a charge carrier concentration of more than $10^{15}\,$cm^{-3} are used as a absorber for photovoltaic IR-detectors with the P^+-n-transition architecture, providing the limiting parameters of IR-detectors at cryogenic and elevated temperatures [7–11].

The lifetime (LT) of minor charge carriers is one of the physical parameters that determines the quality and photoelectric characteristics of IR-detectors. There is an extensive literature on the study of LT in the MCT material with X_{CdTe} $0.2-0.4$ obtained by various methods. When studying the LT in the temperature range from liquid helium to room temperature for different levels of charge carrier concentration, it was found that the main recombination

processes determining the value of the LT in the volume of a direct-gap photonic semiconductor MCT are fundamental Auger and radiation processes and recombination at the Shockley−Hall−Reed (SHR) centers, which are point and structural defects. The surface recombination [12] is also very important in the manufacture of IR-detectors. The LT (τ) at cryogenic temperatures is determined by recombination at the SHR centers, which is inversely proportional to the concentration of such centers (N_{shr}), $\tau \sim 1/N_{shr}$. Despite the abundance of relevant literature, the identity of the SHR centers remains unclear, with the exception of its own defects, residual impurities and complexes [13,14]. It was noted that dislocations can lead to a decrease in the lifetime of [13,15–17].

The surdace or interface recombination between the substrate and the epitaxial layer leads to a decrease in the lifetime, which degrades the parameters of the IR-detector. To reduce or eliminate surface recombination, passivation of the surface is carried out with insulators [18,19], or wideband layers *in situ* [20] are grown on the surface. We have shown that graded wide-band layers at the surface and at the interface between the epitaxial layer and the substrate make it possible to completely exclude the influence of surface recombination on the value of the LT [21,22].

Thus, studies of recombination processes in the HES MCT MBE allowed to obtain, after the growth, of the undoped or indium-doped material *n*-type conductivity with a long lifetime, as on (211)B CdZnTe and (013) GaAs substrates with graded wide-band layers at the boundaries of the absorber layer [23–26]. The undoped layers after growth had *n*-type of conductivity with electron concentration $(2-4) \cdot 10^{14}$ cm^{-3} (for the best samples on CdZnTe substrates $(2-3) \cdot 10^{13}$ cm^{-3}), mobility up to $200\,000$ cm^{2}V^{-1}s^{-1} and lifetime up to $20\,\mu$s at 77 K. In the In$^-$ doped layers, electron mobility and lifetime was in the ranges $100\,000-30000$ cm^{2}V^{-1}s^{-1} and $8.0-0.04\,\mu$s for the In doping level in the range $10^{15}-10^{17}$ cm^{-3}. According to the observed temperature dependence of the LT in the temperature range $77-300$ K, it was found that at electron concentrations below 10^{15} cm^{-3} the values of the measured lifetime are associated with recombination at the centers of the SHR [27]. At higher concentrations, the value of LT is determined by Auger recombination.

For the increasing demand of IR-detectors for various purposes, it is necessary to increase the production of MCT material. Currently, the main high-quality material are the HES MCT on CdZnTe substrates. However, the disadvantages of such substrates associated with their high cost, which increases with increasing size, have led to the development of MOVPE and MBE technologies on alternative substrates of large area GaAs ($\varnothing\,100$ mm) and Si ($\varnothing\,150$ mm). As a rule, these technologies (growth methods) should ensure high uniformity of the parameters of the HES MCT MBE over a large area of structures. However, when developing the technology, heterogeneities of various parameters over the HES area are observed, for some the causes of thier occurrence have been identified

and solutions have been found. In some cases, a large spread of lifetime values over the area (more than an order of magnitude) was observed for undoped the HES MCT MBE. This variation can be explained by the variation in the concentration of SHR centers, which are usually associated with mercury vacancies. The growing conditions are mainly determined by the substrate temperature and mercury pressure in the MBE method, which determine the concentration of mercury vacancies. To obtain a high-quality material, these parameters can change in a narrow range of optimal growing conditions. For large changes in the concentration of mercury vacancies, a wide range of growth conditions is required, which leads to the formation of various well-detectable structural defects with a high density of [14,28,29], which significantly degrades the quality of the HES MCT MBE. However, in some cases, large changes in the lifetime of the HES area are observed with growth in optimal conditions (the ratio of cadmium and tellurium fluxes, mercury vapor pressure in front of the substrate, etc.). In this case, a high concentration of SHR centers providing high recombination velocities is likely to form at certain sections of the HES MCT MBE, which leads to an observed decrease in life time. Currently, the nature of such centers is not defined.

We have conducted studies of the crystal structure of the HES MCT MBE on GaAs substrates by analyzing of the azimuthal dependence of the second harmonic signal of reflected probing laser radiation [30]. For the first time, a quasi-periodic change in the signal in the minimum of the azimuth dependence of the second harmonic was observed over the entire thickness of the MCT layer, exceeding the noise of the receiving path [31]. An assumption was made about the formation of misoriented microregions in the volume during the growth process, which degrades structural perfection. At the boundaries of such misoriented microregions, increased recombination of charge carriers may occur, leading to a decrease in the lifetime of minor carriers.

In this paper, a second harmonic study of the crystal perfection of the HgCdTe layer with an heterogeneous lifetime distribution over the area grown on the substrate (013) GaAs 76.2 mm indiameter by the MBE method is carried out. It is assumed that the possible cause of the observed low values of the lifetime is the recombination processes at new SHR centers, the nature of which is determined by the existence of misoriented microregions of the crystal structure.

2. Samples and experimental procedure

The study of the distribution of electrophysical characteristics and structural perfection of the crystal lattice over area were carried out on a HES MCT MBE sample, grown on a GaAs (013) substrate with diameter of 76.2 mm, with control of the composition and thickness of layers by single-wave ellipsometry *in situ* [24]. When growing

the HES MCT MBE on a prepared atomically clean and smooth [2] surface the buffer layers ZnTe and CdTe and the HgCdTe layer are sequentially grown on the GaAs surface. Figure 1 shows a composition distribution throughout the thickness of the MCT layer of the HES under study 1MCT191113.

The MCT layer with a total thickness of $7.1\,\mu$m includes a homogeneous absorbing layer of the composition of $x = 0.22$, a bottom graded wide-band layer on the interface with a CdTe buffer layer with a change in composition from $x = 0.40$ to $x = 0.22$ throughout the thickness $\sim 0.8\,\mu$m and the upper graded wide-band layer on the surface with a change in composition from $x = 0.22$ to $x = 0.44$ throughout the thickness $\sim 0.4\,\mu$m.

The measurement of the concentration of charge carriers and their mobility of the whole structure and its individual fragments of arbitrary shape which obtained by mechanical separation was carried out by the Van der Pau method at the laboratory Hall effect measurement facility [32,33]. Pressure contacts were used. Measurements of the whole HES MCT MBE were carried out in a vacuum cryostat. Measurements of the HES MCT MBE fragments were carried out when immersed in liquid nitrogen in a special holder with a screen that excludes background illumination. The current through the sample, the magnetic field and the temperature of the measurements were $1\,\mu$A, 0.05 T and 77 K, respectively. The composition, thickness of the MCT layers and their distributions over the area of the structure were determined from the transmission spectra in the wavelength range $2-20\,\mu$m using the Fourier spectrometer „Infralum 801“. The accuracy of determining the composition and thickness of the MCT layers was 0.0005 mole fractions CdTe and $0.1\,\mu$m, respectively.

Lifetime measurements were carried out using a cryostat and a special holder by registering the decay of the microwave photoconductivity signal using the „Tauris-T“ installation at 77 K [34]. The measurements were carried out at a low level of background illumination, the excitation of photoconductivity was carried out by a pulsed semiconductor laser with a wavelength of $0.92\,\mu$m, the decay time of the light pulse (at the level of 0.1) — no more than 10 ns. The diameter of the measured area was 5 mm.

The structural crystal perfection of the substrate and the HES MCT MBE layers was measured at the room temperature by the SHG method *ex situ* on the high-sensitive laboratory test bench for the non-linear optical diagnostics, whose operation is described in detail in [31,35]. The average power of the exciting SH (second-harmonic) YAG:Nd laser varied in the range from 0.01 to 0.07 W. The standard time for obtaining an experimental diagram of the angular dependence of the SH signal ranged from 10 to 30 s. The diameter of the probed area was $200\,\mu$m at the generation depth of SH ~ 5 nm. It should be noted that in the SHG method, a comparative quantitative analysis of experimental and numerical model data for an ideal crystal in a given local region allows us to obtain quantitative information about the crystal state of the near-surface layer
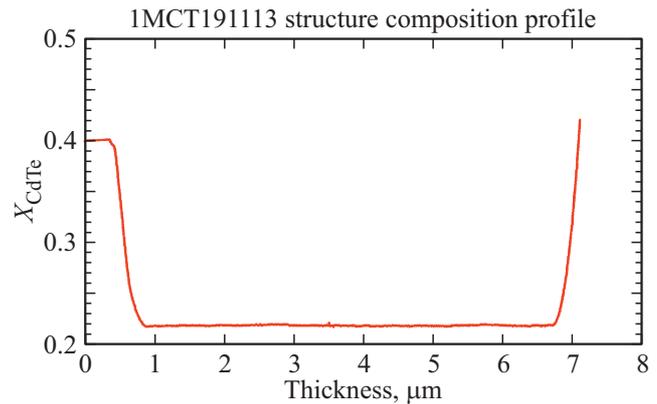
Figure 1. Distribution of the composition X_{CdTe} in the MCT layers of sample 1MCT191113.

of the sample under study [36–38]. Thickness measurements of the crystal state of the MCT layers were carried out with successive layer-by-layer chemical etching in Br:HBr $= 0.05$ solution:1 and measuring the azimuthal dependence of the SH signal intensity.

3. Results and analysis of experimental data

3.1. Model dependence of SH signals in the HES MCT MBE crystals on GaAs substrates in the orientation region (013)

The compounds in the composition of HES MCT MBE and GaAs substrates have a crystal structure of the type of sphalerite of class $\bar{4}3m$. Such crystals do not have an inversion center and belong to nonlinear crystals in which, when exposed to incident radiation with a frequency of ω there is a generation of higher harmonics, including SH with a frequency of 2ω. The calculation of the intensity of the SH signal is carried out using the nonlinear susceptibility tensor $\chi_{xya}(\omega)$ and is described in detail in the works [39,40].

Fig. 2 shows graphs of the model azimuthal dependences of the polarization signal of the SH for an ideal crystal having a symmetry class of sphalerite parallel to the azimuthal polarization angle of the exciting and incident laser radiation normal to the surface, in a laboratory coordinate system with angle variations of φ (counting from orientation (100)) in the orientation region (013). The thick line shows a graph of the azimuthal dependence of the SH signal for a perfectly accurate orientation (013) ($\varphi = 90°$), which represents a periodic change with the same amplitude at the maxima. The azimuthal dependences of the SH polarization signal are shown in thin lines with changes in the angle of φ by one degree in the range from $-10°$ to $+10°$. As can be seen, the neighboring peaks of the SH signal change in the opposite phase — in some the intensity increases, and in others it decreases. From the comparison of experimental and model results, it is possible to determine with high

Composition and electrophysical parameters of fragments of the HES MCT MBE

Sample	Point number (Fig. 3)	Lifetime, μs	Composition, X_{CdTe}	Concentration charge carriers $\times 10^{14}\,cm^{-3}$, (77 K)	Mobility charge carriers $\times 10^3\,cm^2V^{-1}s^{-1}$, (77 K)
1MCT191113	1	1.20	0.222	2.3	63
	2	10.0	0.218	3.15	62
	3	9.00	0.221	2.6	66
	4	12.0	0.220	2.8	64
	5	7.80	0.221	2.6	62
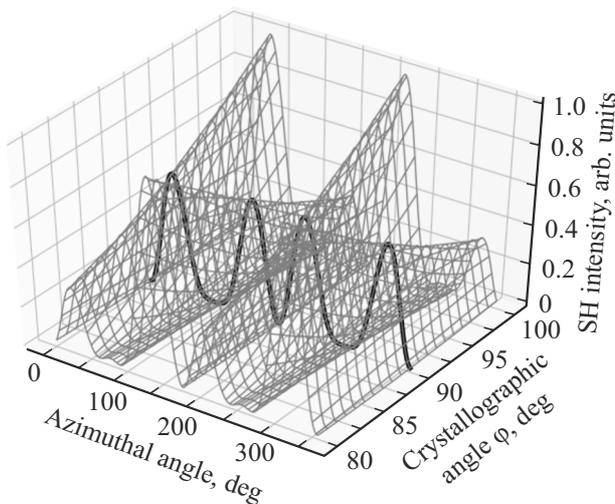
Figure 2. Model surface of the azimutal SH intensity for the normal incident of the beam with the cut variation near (013) by the angle φ. The SH signal polarization is parallel to the polarization of the excitement radiation.

accuracy the rotation of the orientation plane from (013). According to the type of azimuthal dependence of the signal and the emerging features, it is possible to identify stresses or changes in the crystal structure, as well as to analyze possible causes.

3.2. Electrophysical parameters of the HES MCT MBE

Fig. 3 shows the distribution of the lifetime over the area of the HES MCT MBE. It can be seen that a long lifetime from 7.8 to $12\,\mu$s is observed in the edge regions of the structure (points $2-5$), which indicates a high quality of the structure. In the center of the structure (point 1), the lifetime is $1.2\,\mu$s, which is an order of magnitude less than the largest value. In order to identify the reasons leading to the appearance of such a large heterogeneity of the lifetime observed in the studied the HES MCT, it was divided into fragments of about 10×10 mm, including areas in which the lifetime was measured (points $1-5$).

The table shows the data of measurements of the lifetime, composition, concentration of charge carriers and their mobility for the cut fragments.

As it follows from the above data, the composition, concentration of charge carriers and mobility in all fragments of the structure (points $1-5$) have similar values and lie in the intervals $x = 0.218 - 0.221$, $n = (2.3 - 3.15) \cdot 10^{14}\,cm^{-3}$ and $\mu = 62000 - 66000\,cm^2\,V^{-1}\,s^{-1}$. The lifetime of minor carriers in the center of the structure is about an order of magnitude less than at the edges.

3.3. The range of measurement of the azimutal dependence of the second harmonic signal

Figure 4 shows a fragment of the structure and azimuthal dependencies of the second harmonic signal at four points (I−IV) of the surface, including the points 1 and 4 in Figure 3.

In the given data, in the minima of azimuth dependence, beats are observed (highlighted by a dotted oval), which at point I exceed the noise of the measuring path; at point II and III are close to the noise of the measuring path; at point IV correspond to the noise of the measuring path. The beats in the minima of the azimuthal dependence of the second harmonic signal, exceeding the noise of the
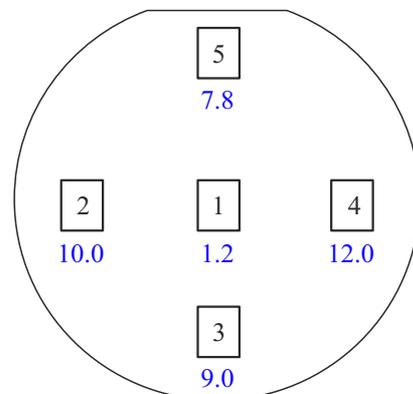
Figure 3. Distribution of the lifetime at 77 K over the area of the HES MCT MBE 1MCT191113. The squares indicate the numbers of the measurement points and the values of the lifetime in microseconds for each point.
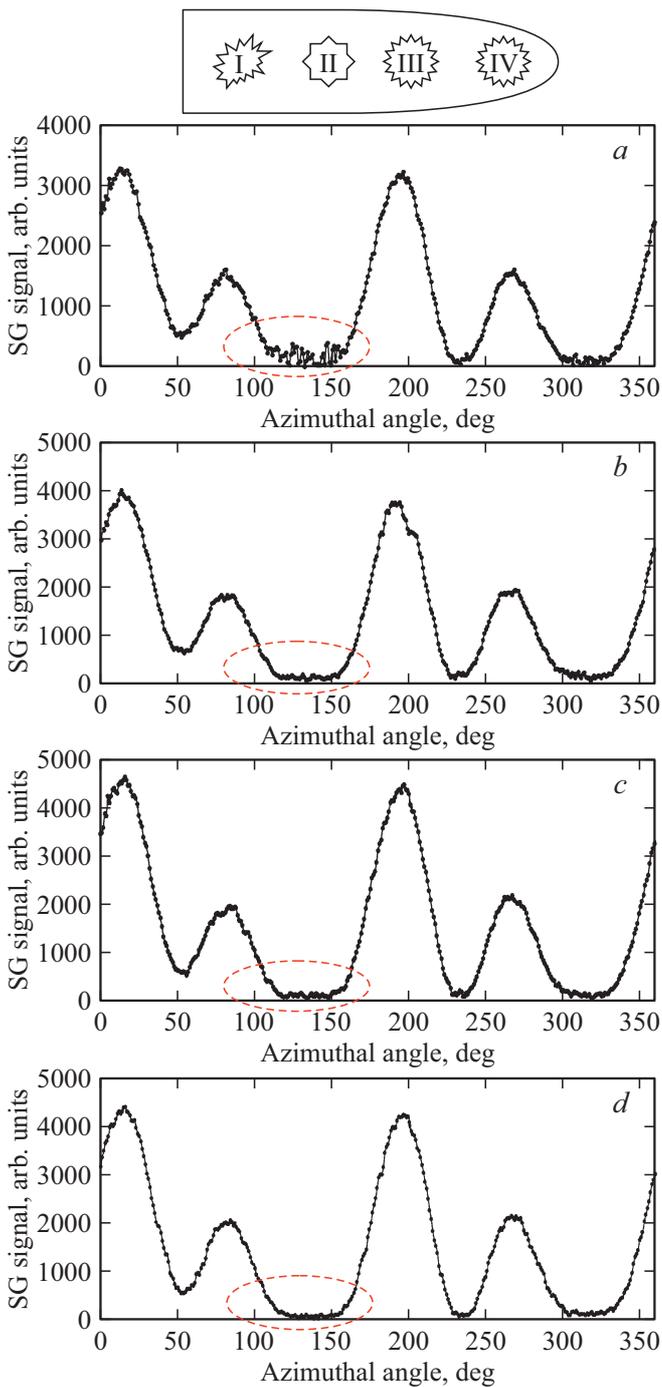
Figure 4. Azimuthal dependence of the second harmonic signal of the fragment HES MCT MBE 1MCT191113 at points I–IV (insert): *a*) — point I (sample center *1*); *b*) — point II (offset from point I by 4 mm); *c*) — point III (offset from point II by 4 mm); *d*) — point IV (edge of sample *4*). *1* and *4* correspond to the points in Fig. 3.

measuring path, we associate with the misoriented microregions that we observed earlier [30]. In this case, during the transition of measurements from point I to point IV, the amplitude of the beats decreases, which corresponds to a decrease in misoriented microregions and its absence

at point 4. After removing the upper graded wide-gap layer when etching the sample to a depth of $1.6\,\mu$m, a similar pattern of changes in the amplitude of the beats in the minima of the azimuthal dependence of the second harmonic signal is observed. Thus, misoriented microregions are present throughout the thickness of the structure and are not associated with a change in composition during the growth of the upper graded wide-gap layer.

It should be noted that the deviation of the orientation of the surface of the structure in the plane of growth (angle φ) is (-6) degrees and does not change for all points I–IV. The magnitude of the amplitude in the maxima of the azimuthal dependence monotonically increases during the transition of measurements from point I to point IV, which can be associated with a change in orientation in a plane perpendicular to the direction of growth (angle θ), by 6 degrees.

3.4. Analysis of the results

When growing HES MCT MBE on substrates of large diameter, more stringent requirements are imposed on the uniformity of parameters over the area. The lifetime is a sensitive parameter that determines the limiting characteristics of IR-detectors. The studies given in the literature of the mechanisms determining the value of the lifetime in the MCT material showed that at 77 K the main mechanism is recombination on SHR centers of various nature. Thus, the presence of mercury vacancies in the MCT (V_{Hg}) determines the strong recombination of SHR and leads to a decrease in the lifetime with an increase in their concentration ($\tau \sim 1/N_{\text{VHg}}$). The observed heterogeneity of the lifetime was an order of magnitude (Fig. 3). To explain this heterogeneity by using V_{Hg} as recombination centers, it is necessary that their concentration varies by an order of magnitude over the area of the structure. Calculations of mercury vacancy concentrations from the substrate temperature and mercury pressure at growth temperatures have shown that in order to change them by an order of magnitude, the temperature must change by $\sim 45°$C and the mercury vapor pressure by an order of magnitude at a temperature $200°$C [41]. Such changes in mercury vapor temperature and mercury vapor pressure are not possible in the MBE method, since the range of these parameters is quite narrow [42,43].

The dislocation density in HES MCT MBE on GaAs (013) substrates is $\sim 10^6\,\text{cm}^{-2}$ [44]. Calculations show that with such a dislocation density in the MCT $x = 0.22$, the lifetime should be $\sim 0.1\,\mu$s. The lifetimes we observe exceed this value by $1-2$ orders of magnitude. Thus, dislocations in the HES MCT MBE do not have a significant influence on the lifetime.

It should also be noted that recombination on the surface or interface does not affect the lifetime in the HES MCT MBE in the presence of graded wide-band layers at the boundaries of the absorbing layer (Fig. 1) [21,22].

The distribution of the composition over the surface is almost uniform and does not exceed $\Delta x = 0.004$ and cannot be the cause of the heterogeneity of the lifetime.

Thus, it is not possible to explain the observed heterogeneity of the lifetime by the reasons given above.

Apparently, the heterogeneity of the lifetime can be associated with changes in the crystal structure of the HgCdTe layer with the growth of HES MCT MBE on GaAs substrate, which may be caused by some heterogeneity of temperature over area or by a different mechanism of nucleation at the initial stage at the edges and in the center of the substrate with the growth of the HgCdTe layer. Indeed, the observed changes in structural perfection, which showed the presence of misoriented microregions (Fig. 4), may be the cause of increased recombination of charge carriers and lead to a decrease in lifetime. Thus, we assume that the emerging misoriented microregions may be the new SHR centers of recombination.

4. Conclusion

The azimuthal dependence of the second harmonic signal of reflected laser radiation in the MCT MBE heterostructures with graded wide-gap layers on GaAs (013) substrates having a heterogeneous distribution of the lifetime of minor charge carriers over the area (from $1.2\,\mu$s to $12\,\mu$s) has been studied. The electrophysical parameters of the fragments of the structure with different lifetimes had similar values: the concentration of charge carriers and mobility in the ranges $(2.3-3.15)\cdot 10^{14}\,\mathrm{cm}^{-3}$ and $62000-66000\,\mathrm{cm}^2\mathrm{V}^{-1}\mathrm{s}^{-1}$, the composition of the MCT absorbing layer in the range with $x = 0.218-0.221$. For the first time, a quasi-periodic signal change was observed in the minimum azimuth dependence of the second harmonic in the region of the structure with a short lifetime over the entire thickness of the MCT layer. It is assumed that the features of the azimuthal dependence of the second harmonic signal are due to misoriented microregions on the surface and in the volume of the MCT layer, which are also new centers of recombination of charge carriers and reduce the lifetime of minor charge carriers.

Conflict of interest

The authors declare that they have no conflict of interest.

References

[1] W. Lei, J. Antoszewski, L. Faraone. Appl. Phys. Rev. **2**, 041303 (2015). DOI: 10.1063/1.4936577.

[2] V.S. Varavin, S.A. Dvoretsky, N.N. Mikhailov, V.G. Remesnik, I.V. Sabinina, Yu.G. Sidorov, V.A. Shvets, M.V. Yakushev, A.V. Latyshev. Optoelectron. Instrument. Proc., **56** (5), 456, (2020). DOI: 10.3103/S8756669020050143

[3] D. K. Arch, R. A. Wood, D. L. Smitha. J. Appl. Phys. **58**, 2360 (1985). DOI: 10.1063/1.33595.

[4] C.A. Musca, J.F. Siliquini, G. Parish, J.M. Dell, L. Faraone. J. Cryst. Growth **184−185**, 1284 (1998), DOI: 10.1016/S0022-0248(98)80266-2.

[5] A.V. Filatov, E.V. Susov, N.M. Akimova, V.V. Karpov, V.I. Shaevich. Uspekhi prikladnoi fiziki **3**, *2*, 96 (2015). (in Russian). PACS: 85.60.Dw

[6] A.V. Filatov, E.V. Susov, V.V. Karpov, A.V. Gusarov. Uspekhi prikladnoi fiziki **9**, *2*, 112 (2021). (in Russian). DOI: 10.51368/2307-4469-2021-9-2-112-127

[7] L. Mollard, G. Destefanis, N. Baier, J. Rothman, P. Ballet, J.P. Zanatta, M. Tchagaspanian, A.M. Papon, G. Bourgeois, J.P. Barnes. J. Electron. Mater. **38**, *9*, 1805 (2009). DOI: 10.1007/s11664-009-0829-9.

[8] D. Eich, W. Schirmacher, S. Hanna, K.M. Mahlein, P. Fries, H. Figgemeier. J. Electron. Mater. **46**, *9*, 5448 (2017). DOI: 10.1007/s11664-017-5596-4.

[9] A.P. Kovchavtsev, A.A. Guzev, A.V. Tsarenko, Z.V. Panova, M.V. Yakushev, D.V. Marin, V.S. Varavin, V.V. Vasilyev, S.A. Dvoretsky, I.V. Sabinina, Yu.G. Sidorov. Infrared Phys. Technol. **73**, 312 (2015). DOI: 10.1016/j.infrared.2015.09.026.

[10] V.S. Varavin, I.V. Sabinina, G.Yu. Sidorov, D.V. Marin, V.G. Remesnik, A.V. Predein, S.A. Dvoretsky, V.V. Vasilyev, Yu.G. Sidorov, M.V. Yakushev, A.V. Latyshev. Infrared Phys. Technol. **105**, 103182 (2020). DOI: 10.1016/j.infrared.2019.103182.

[11] G. Destefanis, J. Baylet, P. Ballet, P. Castelein, F. Rothan, O. Gravrand, J. Rothman, J.P. Chamonal, A. Million. J. Electron. Mater. **36**, *8*, 1031 (2007). DOI: 10.1007/s11664-007-0168-7

[12] A. Rogalski. Infrared detector. 2 nd ed. CRC Press. Tayor& Francis Group, NW. (2011). 876 p.

[13] V.C. Lopes, A.J. Syllaios, M.C. Chen. Semicond. Sci. Technol. **8**, *6S*, 824 (1993), DOI: 10.1088/0268-1242/8/6S/006.

[14] A. Rogalski. Rep. Prog. Phys. **68**, *10*, 2267 (2005). DOI: 10.1088/0034-4885/68/10/R01.

[15] T. Yamamoto, H. Sakai, K. Tanikawa. J. Cryst. Growth **72**, *1−2*, 270 (1985). DOI: 10.1016/0022-0248(85)90156-3.

[16] S.H. Shin, J.M. Arias, M. Zandian, J.G. Pasko, R.E. DeWames. Appl. Phys. Lett. **59**, 2718 (1991). DOI: 10.1063/1.105895

[17] K. Jówikowski, A. Rogalski. J. Electron. Mater. **29**, *6*, 736 (2000). DOI: 10.1007/s11664-000-0217-y.

[18] R. Pal, R.K. Bhan, K.C. Chhabra, O.P Agnihotri. Semicond. Sci. Technol. **11**, 231, (1996). DOI: 10.1088/0268-1242/11/2/015

[19] V. Kumar, R. Pal, P. K. Chaudhury, B. L. Sharma, V. Gopal. J. Electron. Mater. **34**, *9*, 1225 (2005). DOI: 10.1007/s11664-005-0267-2

[20] C.A. Musca, J.F. Siliquini, K.A. Fynn, B.D. Nener, L. Faraone, S.J.C. Irvine. Semicond. Sci. Technol. **11**, *12*, 1912 (1996). DOI: 0.1088/0268-1242/11/12/025

[21] V.M. Osadchy, A.O. Suslyakov, V.V. Vasiliev, S.A. Dvoretsky. Avtometriya. **4**, 71 (1998). (in Russian).

[22] A.V. Wojciechowski, Yu.A. Denisov, A.P. Kohanenko, V.S. Varavin, S.A. Dvoretsky, N.N. Mikhailov, Yu.G. Sidorov, M.V. Yakushev. Avtometriya. **4**, 47 (1998).

[23] D.D. Edwall, M. Zandian, A.C. Chen, J.M. Arias. J. Electron. Mater. **26**, *6*, 493 (1997). DOI: 10.1007/s11664-997-0183-8

[24] Y.G. Sidorov, S.A. Dvorestky, V.S. Varavin, N.N. Mikhailov, M.V. Yakushev, I.V. Sabinina. Semiconductor **35**, *9*, 1045, (2001). DOI: 10.1134/1.1403569

[25] C.H. Swatz, R.P. Tompkins, N.C. Giles, T.H. Myers, D.D. Edwall, J. Ellworth, E. Piquette, J. Arias, M. Berding, S. Krushnamurthy, I. Vurgftman, J.R. Meyer. J. Electron. Mater. **33**, *6*, 728 (2004). DOI: 10.1007/s11664-004-0074-1

[26] B.P. Varavin, S.A. Dvoretsky, D.G. Ikusov, N.N. Mikhailov, Yu.G. Sidorov, G.Yu. Sidorov, M.V. Yakushev. Semiconductors **42**, *6*, 648 (2008). DOI: 10.1134/S1063782608060031

[27] O. Garland. Mercury Cadmium Telluride: Growth, Properties and Applications. Wiley & Sons Ltd., West Susses (2011). P. 131.

[28] C. E. Jones, K. James, J. Merz, R. Braunstein, M. Burd, M. Eetemadi, S. Hutton, J. Drumheller. J. Vac. Sci. Tech. **A3**, 131 (1985). DOI: 10.1116/1.573184.

[29] Yue Fang-Yu, Ma Su-Yu, Hong Jin, Yang Ping-Xiong, Jing Cheng-Bin, Chen Ye, Chu Jun-Hao. Chin. Phys. B **28**, *1*, 017104 (2019).

[30] S.A. Dvoretskiy, M.F. Stupak, N.N. Mikhailov, S.N. Makarov, A.G. Elesin, A.G. Verkhoglyad. Optoelectron. Instrument. Proc. **57**, *458*, 18 (2021). DOI: 10.3103/S8756699021050058

[31] M.F. Stupak, N.N. Mikhailov, S.A. Dvoretskiy, M.V. Yakushev, D.G. Ikusov, S.N. Makarov, A.G. Elesin, A.G. Verkhoglyad. Phys. Sol. State **62**, *2*, 252 (2020). DOI: 10.1134/S1063783420020201

[32] V.S. Varavin, A.F. Kravchenko, Yu.G. Sidorov. Semiconductors **35**, *9*, 992 (2001). DOI: 10.1134/1.1403562

[33] A.V. Vishnyakov, V.S. Varavin, M.O. Gariffulin, A.V. Predein, V.G. Remesnik, I.V. Sabinina, Yu.G. Sidorov. Optoelectron. Instrument. Proc. **45**, *4*, 308 (2009). DOI: 10.3103/S8756699009040049

[34] P.A. Borodovsky, A.F. Buldygin, A.S. Tokarev. Semiconductors **38**, *9*, 1005 (2004). DOI: 10.1134/1.1797476

[35] M.F. Stupak, N.N. Mikhailov, S.A. Dvoretskiy, S.N. Makarov, A.G. Elesin, A.G. Verkhoglyad. ZhTF **91**, *11*, 1799 (2021). DOI: 10.21883/JTF.2021.11.51546.34-21

[36] V.V. Balanyuk, V.F. Krasnov, S.L. Musher, V.I. Prots, V.E. Ryabchenko, S.A. Stoyanov, S.G. Struts, M.F. Stupak, V.S. Syskin. Quantum Electron **25**, *2*, 183 (1995). DOI: 10.1070/QE1995v025n02ABEH000320

[37] P.E. Berezhnaya, M.F. Stupak. Proc. of SPIE **4900**, 98 (2002). DOI: 10.1117/12.484486

[38] G.M. Borisov, V.G. Gol'dort, K.S. Zhuravlev, A.A. Kovalev, S.A. Kochubey, D.V. Ledovskikh, T.V. Malin, N.N. Rubtsova. Sib.fiz.zhurn. **13**, *2*, 64 (2018). (in Russian). DOI: 10.25205/2541-9447-2018-13.

[39] S.A. Akhmanov, V.I. Yemelyanov, N.I. Koroteev, V.V. Seminogov. Sov. Phys. Usp. **28**, 1084 (1985). DOI: 10.1070/PU1985v028n12ABEH003986

[40] T.F. Heinz. Nonlinear Surface Electromagnetic Phenomena. North Holland Pub. (1991). P. 353.

[41] H.R. Vydyanath. J. Electron. Mater. **24**, *9*, 1275 (1995). DOI: 10.1007/BF02653085.

[42] L. He, Y. Wu, L. Chen, S.L. Wang, M.F. Yu, Y.M. Qiao, J.R. Yang, Y.J. Li, R.J. Ding, Q.Y. Zhang. J. Cryst. Growth **227**−**228**, 677 (2001). DOI: 10.1016/S0022-0248(01)00801-6.

[43] Y. S. Ryu, B. S. Song, T.W. Kang, T.W. Kim. J. Mater. Sci. **39**, 1147 (2004). DOI: 10.1023/B:JMSC.0000012966.19192.85.

[44] Y.G. Sidorov, M.V. Yakushev, V.S. Varavin, A.V. Kolesnikov, E.M. Trukhanov, I.V. Sabinina, I.D. Loshkarev. Phys. Solid State **57**, *11*, 2151 (2015). DOI: 10.1134/S1063783415110311